Scanning field emission from patterned carbon nanotube films

L. Nilsson,[a] O. Groening, C. Emmenegger, O. Kuettel, E. Schaller, and L. Schlapbach
Institute of Physics, University of Fribourg, Pérolles, CH-1700 Fribourg, Switzerland

H. Kind, J-M. Bonard, and K. Kern
Department of Physics, EPFL, CH-1015 Lausanne, Switzerland

(Received 6 December 1999; accepted for publication 15 February 2000)

The investigation of the field emission (FE) properties of carbon nanotube (CNT) films by a scanning anode FE apparatus, reveals a strong dependence on the density and morphology of the CNT deposit. Large differences between the microscopic and macroscopic current and emission site densities are observed, and explained in terms of a variation of the field enhancement factor β. As a consequence, the emitted current density can be optimized by tuning the density of CNTs. Films with medium densities (on the order of 10^7 emitters/cm^2, according to electrostatic calculations) show the highest emitted current densities. © *2000 American Institute of Physics.* [S0003-6951(00)00815-9]

During the last decade different forms of carbon thin films, like diamond, diamondlike carbon (DLC), tetrahedral amorphous carbon (ta-C) etc. were found to show extraordinary FE properties from apparently flat surfaces.[1–3] It was believed that the reason for the enhanced FE was related to the electronic properties of the films.[4] This was very promising from a technological point of view since the incorporation of such materials in a gated structure, like a flat panel display (FED), could be done easily over large areas at low cost using standard chemical vapor deposition techniques.[5,6] However there is an increasing number of indications that the enhanced FE is due to intense local electric fields caused by protrusions in the μm and nm range.[7,8]

The production of such protruding field enhancing structures (FES) in gated patterns is a problem of technological relevance.[9,10] To be competitive with more conventional cathodes a cheap and simple technique must thus be developed to reproducibly and selectively deposit carbon FES which, in addition, meet the prerequisites of uniformity ($>10^6$ emitters/cm^2)[6] and current density ($\sim 80\ \mu$A/cm^2).[11]

Recently, a simple nonphotolithographic technique, based on microcontact printing (μCP) of a catalytic precursor, was introduced to fabricate patterned carbon nanotube FES.[12,13] In this letter we report on the field emission properties of patterned FES produced by this technique.

Ethanolic solutions containing 10-60 mM $Fe(NO_3)_3 \cdot 9H_2O$ were used as catalytic inks to be printed on the native oxide of silicon wafers. Samples were then mounted in a tube reactor and CNTs were grown at 720 °C in a mixture of acetylene and N_2.[12,13] The resulting pattern, Fig. 1, is covered by a film of multiwall CNTs, about 15 nm diameter and $\sim 5\ \mu$m height. The width of each line is 10 μm and the distance between the individual lines is 50 μm. An increase of the concentration of $Fe(NO_3)_3 \cdot 9H_2O$ results in an increased density of CNTs on the film, as shown on Figs. 2(a)–2(c).

The samples were investigated by means of a vacuum FE apparatus, which permits integrated FE using a phosphor screen as well as locally resolved FE using a X/Y-scanning tip. With integrated FE, emitter and current density on a macroscopic scale ($\sim$ cm^2) is retrievable. To avoid artifacts due to the sensitivity of the screen, a constant voltage of ~ 3000 V was applied to the screen-anode parallel to our grounded sample, and the field was changed by varying the screen-cathode distance. The X/Y scanning was performed over an area of typically $200 \times 200\ \mu$m^2, divided into 100×100 pixels. The Pt-Ir anode with a tip radius of $2-5\ \mu$m was biased to ~ 100 V. The separation between anode and the surface of the emitting film was fixed at $\sim 3-5\ \mu$m. Extracted FE currents were recorded with a Keithley 237 source-measure unit and plotted as a function of the tip position. The level of the noise was lower than 1 nA during scanning. Contact currents could be distinguished from the FE current by a sudden current increase and saturation of the source-measure device. The base pressure of the FE chamber was better than 10^{-7} mbar.

Integrated FE measurements on patterned samples with various densities of CNTs did not reveal significant differences in their emission properties. All started to emit at low fields ($2-3$ V/μm) but the emission was not homogeneous. As seen in the inset of Fig. 1, the emission was dominated by a comparatively small number (<100) of very strong emitting sites spread out over the entire sample surface.

This indicates that emitters with a lower length-to-diameter ratio (i.e., a lower field amplification factor β) are not detected. Indeed, the number of detectable emission sites depends on the size of the measured surface. A cm^2 area will include very few strong ($\beta \sim 1000$) emitting sites, whereas a local measurement in a $100 \times 100\ \mu$m^2 window may reveal many emission sites with lower β values ($\sim 100-200$) when no strong emitters are present in this window. Furthermore, the resolution of the screen puts a limit to what is detectable on the sample, and emitters with a spatial separation of less than 100 μm are difficult to distinguish. These two facts show that traditional I–V measurements with large area anodes are insufficient for proper FE characterization.

To overcome these difficulties we performed FE scans with a Pt-Ir tip and found indeed that there are in fact large

[a]Electronic mail: Lars-Ola.Nilsson@unifr.ch

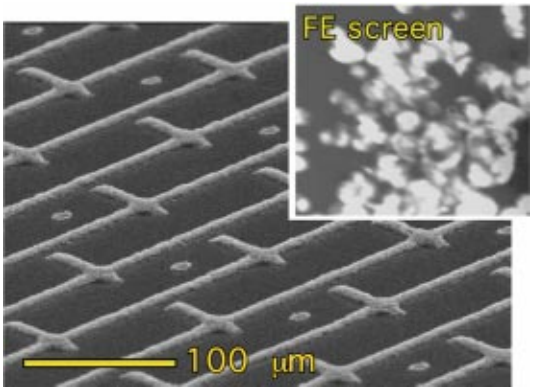

FIG. 1. (Color) Low magnification SEM image of a CNT sample printed with an ethanolic solution of 40 mM $Fe(NO_3)_3 \cdot 9H_2O$. The inset shows a macroscopic emission image of $2.5 \times 2.5\ mm^2$ on the phosphor screen at 5 V/μm.

differences between different samples. In Fig. 2 we compare three FE scans on patterned samples with different densities of CNTs with the corresponding morphology seen in scanning electron microscopy (SEM). Figure 2(d) shows the emission from a high-density CNT sample and is characterized by a rather inhomogeneous emission pattern. The lines and a few crosslines are recognizable, but a clear emission pattern is not obtained. A similar result [Fig. 2(f)] applies to the low density CNT sample, but the emission intensity is

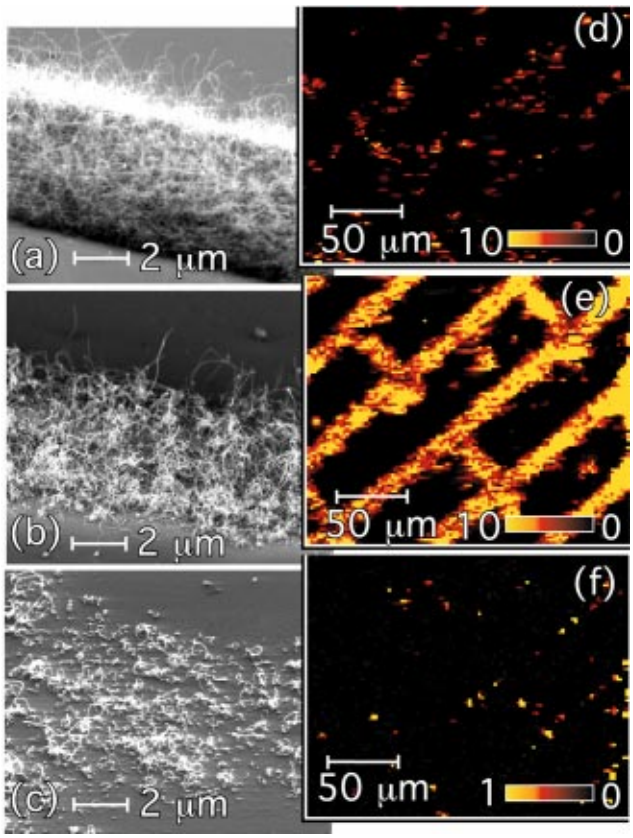

FIG. 2. (Color) SEM images of patterned CNT films showing regions of (a) high, (b) medium, and (c) low density, with the corresponding FE maps of current density (d)–(f). The films were produced with ethanolic inks of 10 (a), 40 (b), and 60 mM $Fe(NO_3)_3 \cdot 9H_2O$. The FE maps were taken under identical conditions using 100 V in constant voltage mode. The color scale corresponds to 0-10 μA/pixel for images (d), (e); and to 0–1 μA/pixel in image (f).

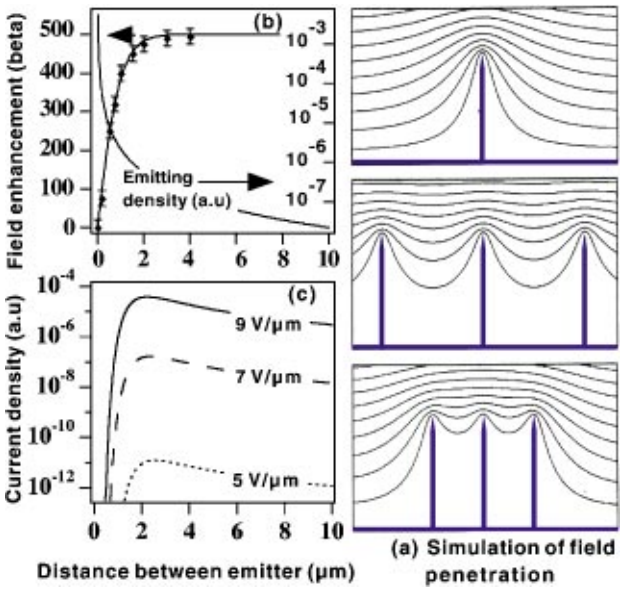

FIG. 3. (Color) (a) Simulation of the equipotential lines of the electrostatic field for tubes of 1 μm height and 2 nm radius, for distances between tubes of 4, 1, and 0.5 μm; along with the corresponding changes of the field enhancement factor β and emitter density (b), and current density (c) as a function of the distance.

lowered by a factor of 10 and the pattern is even less pronounced. For the pattern with a medium CNT density, a much better emission image [Fig. 2(e)] is obtained: lines, crosslines, and dashes can be easily distinguished. Emission from this sample and on this scale is very homogeneous.

The obtained emission behavior is a combination of two effects. The poor emisson of high density films, as in Fig. 2(d), are explainable by an electrostatic screening effect provoked by the proximity of neighboring tubes. The solution of the Poisson equation governs the behavior of the potential penetration into the CNT deposit. The presence of many tubes per unit area (u.a.) means that there is more charge per u.a. and the charge reduces the potential drop perpendicular into the film. Since it is the local electric field ($\sim 3000-4000$ V/μm) at the emission site that governs the emission, the distance between the tubes remains a crucial parameter to optimize the FE. The limit of zero distance between the tubes would correspond to a flat metal surface without field penetration. The film depicted in Fig. 2(a) is close to this limit since the CNTs are densely packed. In fact, we observe some FE only because there are a few tubes that are branching out of the pattern. Low density films [Fig. 2(c)] also give poor emission but for another reason. As seen in the SEM image, the CNTs are short, bent, and not protruding out of the substrate. Only very few of them have a sufficient β factor for an adequate emission. Thus the morphology of individual tubes is indeed of crucial importance for the FE properties. We conclude that a film with a medium density of high aspect ratio tubes shows optimal FE performance. These conditions are best fulfilled for the sample of Fig. 2(b).

In order to verify our experimental findings we performed electrostatic calculations of the field penetration between parallel standing tubes, as shown in Fig. 3(a). We assumed tubes of 1 μm length with a tip apex of 2 nm and decreased the distance between the tubes. The equipotential lines and thus the field enhancement factor β are seen to be

strongly affected as the intertube distance is decreased. The field enhancement factor β is displayed as a function of the distance in Fig. 3(b), along with the density of emitting sites. Inserting β and emitter density into the Fowler-Nordheim equation yields the current density as a function of the distance and applied macroscopic field, shown in Fig. 3(c). In accordance with the experiment we find an optimum intertube distance of 2 μm where the emission is strongest. It is worth noting that this effect is dominated by the field penetration, which is determined by the relative height of the CNTs compared to the intertube distance. A variation in the tube tip apex changes the magnitude of the field amplification but does not influence significantly the optimum distance.

By comparing the current density versus distance in Fig. 3 with the FE maps of Fig. 2, we conclude that three different emission regimes can be defined. Emission from low density CNT films is poor because there are few emitting sites of unsufficient β factors, whereas emission from densely packed CNT films is poor because of reductions in the field enhancement factor due to screening effects. In the intermediate regime, the distance between CNTs is sufficient to reach substantial local fields, and the available emitter density is still sufficient for adequate emission currents.

In summary, completely different values of current and emitter density are obtained using a screen technique as compared to a scanning tip technique. The reason for the discrepancy is found in the composition of few high β emitters ($\beta \sim 1000$) and a majority of low β emitters ($\beta \sim 100$). When our samples are measured with a large anode, the emitters with the highest β dominate the emission. Since they represent a very small fraction of all possible emitters, the emission is not homogeneous and the obtained current densities are low. When microscopically investigated, the low β emitters are also recorded and much higher local current densities, $\sim 100\ \mathrm{A/cm^2}$, are observed from individual pixels as seen in Fig. 2(e). Local current densities are thus a factor 10^5 higher than during macroscopic FE and it appears that an improved monodispersivity of the β factors is necessary to obtain homogeneous high currents over a large anode. We have shown experimentally and theoretically that the density of the nanotubes plays a crucial role for the FE properties. CNT films of low density yield low currents essentially because the emitter density and the β factor are low. For high density films, screening effects reduce the field enhancement and thus the emitted current. For films of medium density, there is an ideal compromise between the emitter density and the intertube distance, which is sufficiently large to avoid screening effects. A better control of density and morphology (and hence of the β factors) of the films is thus clearly required for future applications. Our calculations predict that an intertube distance of about 2 times the height of the CNTs optimizes the emitted current per unit area. For straight tubes of 1 μm height, this would correspond to an ideal density of 2.5×10^7 emitters/cm^2, or equivalently to ~ 625 emitters per $50\times50\ \mu\mathrm{m}^2$ pixel.

This work was supported by Motorola and NFP 36 of the Swiss National Science Foundation.

[1] C. Wang, A. Garcia, D. C. Ingram, M. Lake, and M. E. Kordesch, Electron. Lett. **27**, 1459 (1991).
[2] G. A. J. Amaratunga and S. R. P. Silva, Appl. Phys. Lett. **68**, 2529 (1996).
[3] O. Gröning, O. M. Küttel, P. Gröning, and L. Schlapbach, Appl. Surf. Sci. **111**, 135 (1997).
[4] M. W. Geis, J. C. Twichell, and T. M. Lyszcyarz, J. Vac. Sci. Technol. B **14**, 2060 (1996).
[5] J. E. Jaskie, MRS Bull. **21**, 59 (1996).
[6] R. L. Fink, Z. Tolt, and Z. Yaniv, Surf. Coat. Technol. **108/109**, 570 (1998).
[7] O. Gröning, O. M. Küttel, P. Gröning, and L. Schlapbach, J. Vac. Sci. Technol. B **17**, 1064 (1999).
[8] J.-M. Bonard, J. P. Salvetat, T. Stöckli, W. A de Heer, L. Forró, and A. Châtelain, Appl. Phys. Lett. **73**, 918 (1996).
[9] S. Fan, M. G. Chapeline, N. R. Franklin, T. W. Tombler, A. M. Cassell, and H. Dai, Science **283**, 512 (1999).
[10] Z. F. Ren, Z. P. Huang, D. Z. Wang, J. G. Wen, J. W. Xu, J. H. Wang, L. E. Calvet, J. Chen, J. F. Klemic, and M. A. Reed, Appl. Phys. Lett. **75**, 1086 (1999).
[11] J. E. Jaskie (private communication).
[12] H. Kind, J-M. Bonard, C. Emmenegger, L. O. Nilsson, K. Hernadi, E. Maillard-Schaller, L. Schlapbach, L. Forró, and K. Kern, Adv. Mater. **11**, 1285 (1999).
[13] H. Kind, J-M. Bonard, L. Forró, K. Kern, K. Hernadi, L. O. Nilsson, and L. Schlapbach (unpublished).